International Journal of Engineering and Advanced Technology (IJEAT)
ISSN: 2249-8958 (Online), Volume-4 Issue-6, August 2015

Performance of Nano–Modified Cement Pastes and Mortars in Caron's Lake Water

Saleh Abd El-Aleem Mohamed, Wafaa Mohamed Morsi

Abstract: Nanomaterials (NMs) are gaining widespread attention to be used in construction sector so as to exhibit enhanced performance in terms of smart functions and sustainable features. The understanding of complex structure of cement based materials at nano-level will definitely result in a new generation of stronger and more durable concrete; with high range of newly introduced properties. This work aims to study the effect of nano-silica (NS) on hydration characteristics, mechanical, microstructure and durability of OPC-slag-NS cement pastes and mortars subjected to Caron's Lake water. The hydration characteristics were followed by estimation of setting times, chemically combined water, free lime, total chloride and sulphate contents, as well as bulk density, compressive and flexural strengths. The hydration process and durability of cement pastes were monitored using SEM and XRD. The results of these investigations indicate that, NS improves the compressive and flexural strengths of cement specimens subjected to Caron's Lake water up to 12 months. The accumulation of additional hydration products within the pore system enhances the densification of cement paste matrix to form closed structure with narrow pores. NS decrease the accessibility of SO_4^{2-} and Cl^- to penetration into the pore system to form ettringite and chloroaluminate hydrate, hence the total sulfate and total chloride contents decrease with NS content. Mortars containing 4 mass, % NS possess higher values of compressive and flexural strengths than those of the other mortars containing NS. Partial inhibition of chloroaluminate formation and the fine closed microstructure of composite cement containing NS caused an increase of compressive and flexural strengths.

Keywords: Slag, Nano-silica, cements, Mechanical properties, Durability

I. INTRODUCTION

With the expected increase in cement production to meet the need of steadily growing world population and with the urgent need to reduce the amount of energy consumed and CO_2 released in the air, there will be an increasing pressure to reduce cement consumption. The problem of producing blended cements has been of considerable scientific and technological interest, because they need less energy for production **[1]**. In these cements, the mineral admixtures such as fly ash (FA), silica fume (SF), granulated blast-furnace slag (GBFS) and metakaolin (MK) are commonly used as a partial substitution of Portland cement. These admixtures are often added to lower the heat of hydration of cement, decrease the impermeability, and improve the durability and consequently modifying the physical, chemical and engineering properties of concrete **[2–4]**.

Manuscript published on 30 August 2015.
***** Correspondence Author (s)
Saleh Abd El-Aleem Mohamed*, Department of Chemistry, Faculty of Science, Fayoum University, Fayoum, Egypt.
Wafaa Mohamed Morsi, Building Physics Institute BPI, Housing and Building National Research Center, HBRC, Dokki, Giza 11511, Egypt.

GBFS has been used for many years as a supplementary cementitious material (SCM) in concrete, either as a mineral admixture or a component of blended cement. GBFS typically replaces 35–65 mass% of Portland cement (OPC) in concrete. Thus 50 mass, % replacement of OPC would result in a reduction of many thousands of tons of CO_2 over the world of cement production **[5, 6]**. GBFS is a by-product formed in the iron manufacture from the fusion of limestone with ash from coke and the siliceous and aluminous residue remaining from the iron ore after the reduction to iron metal. In this process, a molten slag forms as nonmetallic liquid that floats on the top of the molten iron. It is then separated from the liquid metal and cooled. Depending on the cooling mode, three types of slag are produced, i.e., air-cooled slag (ACS), expanded or foamed slag and granulated slag **[7, 8]**. The rapid cooling of molten slag by water prevents the formation of large crystals, and the resulting slag normally contains more than 95% of glass (amorphous calcium aluminosilicates). This type of slag is called GBFS or water-cooled slag (WCS) **[9]**. Nanotechnology (NT) has changed our vision, expectations and abilities to control the material world. Nanomaterials (NMs) are gaining widespread attention to be used in construction sector so as to exhibit enhanced performance in terms of smart functions and sustainable features. Better understanding of complex structure of cement based materials at nano-level will definitely result in a new generation of stronger and more durable concrete, with the whole range of newly introduced properties **[10]**. Actually, NMs can change the concrete world, due to their unique physical and chemical properties, which different from those of the conventional materials **[11]**. The fundamental processes that govern the concrete properties are affected by the performance of the material on nano-scale. The main hydration product of cement-based materials, the C–S–H gel, is a nano-structured material **[12, 13]**. The mechanical properties and the durability of concrete mainly depend on the refinement of the microstructure of the hardened cement paste and the improvement of the paste-aggregate interfacial transition zone (ITZ) **[14]**. During the last decade, NMs such as nano-SiO_2 (NS), TiO_2 (NT), Al_2O_3 (NA), Fe_2O_3 (NF), ZnO (NZ) and carbon nano-tubes (CNTs) are commonly used in cement products. NS has been used most extensively in cementitious system **[15]**, due to the highly pozzolanic activity, which results in the formation of hydrated silicates with densified microstructure **[16-20]**. Nano-SiO_2 enhances the compressive strength, reduces the permeability and consequently improves the overall durability of hardened concrete **[21, 22]**.

Published By:
Blue Eyes Intelligence Engineering and Sciences Publication (BEIESP)

Concrete is termed durable when it keeps its form and shape within the allowable limits when exposed to different environmental conditions. Over the last few decades, the concrete durability has been a major concern of civil engineering professionals, a considerable scientific and technological interest, because sea structures are exposed to simultaneous action of chemical deterioration processes as a result of the harmful combined effects of the chemical action of seawater constituents on cement hydration products and the corrosion of reinforcing steel. The sulphate and chloride ions from the environment can enter into deleterious reactions leading to the dissolution of CH and precipitation of gypsum and sulfoaluminates (ettringite and monosulfate) as well as chloroaluminate (Friedel's salt), which cause expansion and softening of concrete, respectively **[23-25]**. The $CaCl_2$, which is formed from the reaction of $MgCl_2$ with liberated lime increases the leaching and thus increases the porosity of concrete, leading to stiffness and strength loss. $Mg(OH)_2$ dissociates C–S–H produces CH and silica gel **[26]**. The latter may react with $Mg(OH)_2$ to form magnesium silicate hydrate (Mg–S–H). Also, C–S–H in hydrated cement is decomposed by $MgSO_4$ in aggressive solutions to give gypsum, hydrated silica and Mg–S–H, but the later, unlike silica gel, has little or no binding properties. MgSO4 has a more aggressive effect than Na_2SO_4, because $MgSO_4$ decomposes the C–S–H during long-term exposure to produce Mg–S–H and CH. The presence of Mg^{2+} as $MgSO_4$ or/and $MgCl_2$ leads to the distortion of C–S–H through a dissolution of Ca^{2+} or/and an exchange with Mg^{2+} to give also Mg–S–H and CH. All the above mentioned reactions are accompanied by decrease in strength**[27]**.Calcium, sodium, magnesium and ammonium sulphates constitute hazards to concrete as they react with hydrated cement paste leading to expansion, cracking, spalling and loss of strength **[23]**. The chemical resistance of blended cements results mainly from the pozzolanic reaction, which leads to the consumption of free lime and formation of additional amounts of calcium silicate and aluminosilicate hydrates. These products fill up the open pores, leading to the formation of more homogeneous and compact microstructure. Therefore, the blended cement specimens resist sulphate and chloride attack. Despite the presence of several studies describing the main properties and characteristics of concrete containing NS particles, most of them focus on the application of NS and concrete durability **[28–34]**. This work aims to study the characteristics and durability of NS-blended cements in Caron's Lake water.

II. MATERIALS AND EXPERIMENTALS

II (A). Materials

The starting materials used were ordinary Portland cement (OPC), granulated blast-furnace slag (GBFS), nano-silica (NS) and polycarboxylate superplasticizer. OPC was provided from Beni-Suief Portland Cement Company and GBFS was supplied from Iron and Steel Company, Helwan, Egypt. Their chemical analyses are given in Table 1. The Blaine surface area of OPC and GBFS were 3050 and 4000 cm^2/g, respectively. NS with the average particle size of 15 nm, 99.9 purity% was supplied from nano-technology laboratory, Faculty of Science, Beni-Suief University, Beni-Suief, Egypt. XRD, TEM and SEM of NS are given in Figs.1 and 2. Conplast SP-610 superplasticizer was obtained from Fosroc Company, 6 October City, Egypt. It is an opaque light yellow liquid with density 1.08 g/ml and chloride content < 0.1 mass%.

II (B). EXPERIMENTALS

The cement blends were mixed in a rotary mixer according to the following sequence: (i) NS was stirred with 1.0 % superplasticizer and 25% of mixing water at high speed of 120 rpm for 2 min, (ii) the cement and the residual amount of mixing water were added to the mixer at medium speed (80 rpm) for 1 min, (iii) the mixture was allowed to rest for 90 second and then mixed for 1 min at high speed. For preparation of the mortars, the sand was added gradually and mixed at medium speed for additional 30 second after step (ii). The mortars were prepared by mixing 1 part of cement and 2.75 parts of standard sand proportion with water content to obtain a flow of 110±5 with 25 drops of the flowing table **[27]**. Freshly prepared cement mortars were molded in 50×50×50 mm cubic molds. The molds were vibrated for few minutes for better compaction. The mix compositions of the prepared cement blends are given in Table 2. The samples were cured under tap water for 28 days (zero time), then immersed in Caron's Lake water for 1, 3, 6, 9 and 12 months. The chemical analysis of Caron's Lake water was reported in earlier publications **[24, 27]**. The required water of standard consistency and setting times for each mix were determined according to ASTM specification **[35]**. The hydration of cement pastes were stopped by pulverizing 10g of representative sample in a beaker containing 1:1 methanol–acetone mixture, then mechanically stirred for 1h. The mixture was filtered through a G4, after washing two times with the stopping solution and diethyl ether, then dried at 70ºC for 1h, then collected in polyethylene bags; sealed and stored in desiccators for analysis **[36]**. The combined water content is considered as the percent of ignition loss of the dried sample (on the ignited weight basis). Approximately 2g of the pre-dried sample were ignited up to 1000ºC for 1h soaking time. The results of combined water contents were corrected for the water of free lime present in each sample **[24]**. Free lime contents of the hydrated cement pastes can be thermally determined. 0.5g sample of the hardened cement was placed in a porcelain crucible introduced into a cold muffle furnace. The temperature was increased up to 390, then to 550ºC at heating rate of 3ºC /min. The loss of weight occurred between 390 and 550ºC with soaking time of 15 min is equal to the weight of water of calcium hydroxide. Therefore, the free Portlandite can be calculated **[37]**. pH-value of hardened cement paste was estimated by placing about 10 g of pre-dried specimen into 100 ml of distilled water, then stirring at room temperature for 30 min using a magnetic stirrer. PH-value was measured using pH-meter, Schott. GLAS Mainz-Type CG 843-Germany. The bulk density was carried out before the specimens subjected to the compressive strength determination. Each measurement was conducted on at least three similar cubes of the same mix composition and curing time, then the density can be determined **[27]**.

Published By:
Blue Eyes Intelligence Engineering
and Sciences Publication (BEIESP)

Compressive strength was determined according to (ASTM Designation: C-150, 2007) **[38]**, a set of three cubes was tested on a compressive strength machine of SEIDNER, Riedinger, Germany, with maximum capacity of 2000 KN force. The total sulfate content was gravimetrically estimated by using 1g sample dissolved in 5 ml of concentrated HCl and 100 ml of distilled water were added, then boil for 5 minutes, filter and wash several times with distilled water. Add to the filtrate 10 m1 of 10% $BaCl_2$, digest, filter and ignite at 1000ºC for 30 minutes. The total sulfate content was calculated as:

$$SO_3, \% = \frac{\text{weight of ppt.}}{M} \times 34.3$$

Where, M is the weight of sample in grams. Total chloride was determined by weight 2 g into a stopper conical flask, dispersed with 25 ml water and then added 10 ml of nitric acid (sp. gr. 1.42). Add 50 ml hot water, heat to near boiling and keep warm for 10 to 15 minutes. If the supernatant liquid is turbid, filter through filter paper (41) and wash with hot water, then cool to room temperature. An excess of standard 0.1N AgNO3 was added and 2-3 ml of nitrobenzene to coagulate the precipitate, stopple the flask and shake vigorously, then add 1 ml of ammonium ferric alum as indicator and titrate against standard 0.1 N ammonium thiocyanate **[24 & 27]**. The powder method of X-ray diffraction (XRD) was adopted in the present study. For this, a Philips diffractometer PW 1730 with X-ray source of Cu kα radiation (λ=1.5418Å) was used. The scan step size was 2θ, the collection time 1s, and in the range of 2θ from 5 to 65o. The X-ray tube voltage and current were fixed at 40 KV and 40 mA respectively. An on-line search of a standard database (JCPDS database) for X-ray powder diffraction pattern enables phase identification for a large variety of crystalline phases in a sample. The morphology of the hydration products was investigated through ESE-MEDX after specified hydration times were investigated by ESEM ''Inspect S'', FEI Holland.

III. RESULTS AND DISCUSSION

III (A). The required water of standard consistency and setting times

The required water of standard consistency, initial and final setting times of the prepared OPC-GBFS-NS composite cement pastes are graphically represented in Fig. 3. It can be seen that the required water of standard consistency of M1 (55% OPC, 45% GBFS, 0% NS) decreases, whereas the initial and final setting times elongated, this is due to the lower hydraulic reactivity of GBFS in comparison with OPC during the very early ages of the hydration; this is due to the formation of acidic oxide film formation on the outer most layers of slag grains. The required water of standard consistency and setting times of OPC-GBFS-NS composite cement pastes increases with NS content **[39]**. Replacement of NS instead of OPC increases of the required water of standard consistency; this is due to high surface area of NS. Initial and final setting times are elongated with NS content. The retardation of the setting processes is due to presence of 1% polycarboxylate superplasticizer as well as the excess of mixing water required for standard consistency **[40]**.

III (B). Chemically combined water contents

The variations of the chemically combined water contents with curing time of all hardened composite cement pastes in comparison with SRC pastes immersed in Caron's Lake water for 0, 1, 3, 6, 9 and 12 months are graphically represented in Figure 4. Chemically combined water contents increases with the increase of curing ages for all hydrated cement pastes. This is mainly due to the continuous hydration of the cement clinker phases to form more hydrated products, which deposited in the available open pores. Generally, the chemically combined water contents show a higher increase up to one month; this is mainly due to the acceleration effect of $MgSO_4$ and $MgCl_2$ on the hydration of cement **[24]**. Mix M1 gives lower chemically combined water contents than those of mix M0. The values of chemically combined water contents of specimens cured in Caron's Lake water for 12 months increases with NS content up to 4%. NS particles accelerate the hydration of cement, due to the higher activity and higher surface area **[41]**. The composite cement paste containing 4 mass, % NS (M5) has the highest values of chemically combined water content up to 12 months. NS reacts with the liberated CH during the hydration of cement phases to form additional hydrated products such as C-S-H and C-A-S-H. The values of chemically combined content decreases with 5-6% NS (M6 and M7), but still higher than M0 and M1 pastes.

III (C). The free Portlandite contents and pH values

The free Portlandite contents and pH values of the different hardened cement composite pastes containing NS immersed in Caron's Lake water up to 12 months are plotted against curing time in Figs. 5 and 6. The free Portlandite contents and pH values of composite cement pastes decrease with curing time for all composite cement pastes up to 12 months, this is due to the pozzolanic reaction of both GBFS and NS with the liberated free portlandite from the hydration of OPC cement clinker phases (β-C_2S and C_3S). As NS content increases, the values of free Portlandite contents and pH values decrease, due to the higher pozzolanic activity of NS. Therefore, the addition of NS in the presence of 1% superplasticizers tends to form dispersed-hydrated products with low C/S and low $Ca(OH)_2$ content, leading to form homogeneous composites. Pozzolanic C–S–H gels have a lower Ca/Si ratio and different gel porosities as shown in the pore structure of composite cement with slag and nano-silica addition were reported in **[42, 43]**. The combination of superplasticizer and NS the microstructure displayed a more denser arrangement of microcrystalline CSH as the main hydration products with minor or nil amounts of $Ca(OH)_2$. The addition of nano-silica promotes the densification of the cement matrix. Despite this densification, the apparent porosity of paste increases with the addition of nano-silica, similarly to the results obtained for the porosity of superplasticized pastes. NS made the pore structure of paste more homogeneous by increasing medium capillary porosities. The increased gel porosity can be caused by an increase in the amount of C–S–H gel in the paste; this is due to the acceleration effect of the nano-silica **[17]**.

Published By:
Blue Eyes Intelligence Engineering and Sciences Publication (BEIESP)

The increased gel porosity could result from a higher hydration degree and from the properties of the gel produced by the pozzolanic reaction of the nano-silica particles. As the NS content increases, the values of both free Portlandite contents and pH values decrease, due to the higher pozzolanic affinity of NS in comparison with GBFS **[16]**. This indicates that cement pastes containing different contents of NS were more durable in Caron's Lake water than OPC pastes, this is due to the formation of additional amounts of calcium silicate hydrates, which were formed by pozzolanic reaction filling the available pores and leading to restrict of the penetration by the aggressive ions ($SO4^{2-}$ and Cl^{-}) **[27]**. OPC cement paste had the highest value of free lime. The Portlandite contents of the OPC pastes decreased with curing time up to 3 months and then increased up to 1 year. The decrease of free Portlandite contents was mainly due to the reaction with $MgCl_2$ and $MgSO_4$ forming $CaCl_2$, $CaSO_4$ and $Mg(OH)_2$. Magnesium ion form a layer of brucite at the exposed surface in presence of free lime, because of the low solubility of brucite, the penetration of Mg^{2+} beneath the brucite layer into the interior of the paste is restricted. The brucite formation consumes a high amount of free lime released from hydration. Once the available $Ca(OH)_2$ is depleted**[44]**. Furthermore, the presence of sodium chloride increased the solubility of $Ca(OH)_2$ **[24, 27]**. The increase of Portlandite of OPC pastes after 3 months up to 1year. $Mg(OH)_2$ dissociated C-S-H and produced $Ca(OH)_2$ and silica gel. Silica gel reacted with $Mg(OH)_2$ to form magnesium silicate hydrates, which led to the increase of free lime content **[45]**.

III (D). Compressive, flexural strengths and Bulk density

Compressive, flexural strengths and bulk density of hardened composite cement mortars containing NS in comparison with OPC mortars immersed in Caron's Lake water up to 12 months were graphically represented in Figs.7-9. The results showed that the compressive, flexural strengths and bulk density of all composite cement mortars containing different contents of NS increased up to 1 year. In contrast, the compressive strength, flexural strength and bulk density of OPC mortar (M0) increased up to 3 months, whereas these values corresponding of mix (M1) increase up to 6 months and then decreased up to 12 months. The increase of compressive strength of cement mortars up to 3 or 6 months is due to the acceleration effect of sulfate and chloride ions on the hydration of cement phases, which led to form calcium silicate and calcium sulphoaluminate hydrates. The amount of C–S–H increased greatly during the first 3 months of hydration; therefore the compressive strength was enhanced. The mixture M1 has a higher compressive strength than OPC mortars when immersed in Caron's Lake water, this is due to the pozzolanic reaction of GBFS that helped in the formation of a denser structure, the amount of C-S-H increases during the first 6 months, as well as due to the acceleration effect of $MgSO_4$ and $MgCl_2$ on the hydration of cement. Parts of the Mg^{2+} ions is adsorbed and incorporated into the particles of calcium silicate hydrates. This process stabilizes and enhances its crystallization as well as strength of cement pastes. NaCl presents in Caron's Lake water increases the solubility of $Ca(OH)_2$, which increases the stability of calcium silicate hydrates and consequently the strength of the cement mortars increases. On one hand, a part of the Na^{+} tends to be absorbed by the particles of C-S-H and to be incorporated into its interlayer space **[24, 26]**, to give better ordered calcium silicate hydrates that formed and the strength increases. On the other side, the decrease of compressive strength after the first 6 months and up to one year is mainly due to the aggressive attack of chloride and sulphate ions containing Caron's Lake water. The results indicate that, the compressive and flexural strengths are improved with curing age. The reactivity of NS is controlled by its specific surface area and the amount of Q2-3 (silanol) Si–OH groups, which cover the NS particle. These groups constitute condensation sites for monomeric silica units released from the cement clinker phases; consequently, the hydration of the cement mortars is accelerated **[28]**. The strong and instantaneous interaction between NS and liberating Portlandite leading to the formation and accumulation of excessive amounts of hydrated products mainly as CSH, which fill the pore system and tend to increase the gel/space ratio, causing packing effect. The compressive and flexural strengths of cement mortars containing NS are higher than those of M0 and M1. The results show also that the compressive and flexural strengths of the investigated specimens increase with NS up to 4 mass, % NS. Mortars containing M5 possess higher values of compressive and flexural strengths than those of the other mortars. The addition of NS tends to improve the durability of OPC cements mortars in aggressive solution. This is attributed to the effect of NS, which behaves not only as a filler to improve microstructure, but also as an activator to promote pozzolanic reaction as well as acts as nucleating sites to form more accumulation and precipitation of calcium silicate, aluminate and alumino-silicate hydrates in the open pores originally filled with water, leading to the formation of homogeneous, dense and compact microstructure. OPC cements mortars give the lower compressive strength values at all immersing ages, this is mainly due to the high content of Portlandite, which formed during the hydration. As a result of this $CaCl_2$ and $CaSO_4$ are formed. The chloro- and sulphoaluminate hydrates are formed, which make softening and expansion. The penetration of sulphate ions into the mortars would result in conversion of calcium aluminate hydrate and monosulphate aluminate hydrate into ettringite, which expands resulting internal stresses, cracking and deterioration of cement mortars. $MgCl_2$ also reacts with $Ca(OH)_2$ forming $CaC1_2$ and $Mg(OH)_2$. Calcium chloride reacts with calcium aluminate hydrates producing calcium chloroaluminate hydrates, which has deleterious effect on cement that decrease in the strength after 3 or 6 months up to 12 months for M0 and M1 respectively. Very fine NS with high surface area, improves the packing of particles at the surface of the cement grains, which also favors the pozzolanic reaction, i.e. the formation of denser and high stiffness C–S–H phases **[19, 40, 46]**. The changes in the microstructure in the presence of NS is responsible for the highly increase in compressive strength. Composite cement mortars containing NS showed higher values of compressive and flexural strengths, due to the decreased accessibility of sulfate and Chloride ions towards the more dense structure and low capillary pore structure of the hardened pastes during prolonged hydration. It can be concluded that mix M.5 is the optimum mix which has a high durability and can resist the effect of the sulfate and chloride attack.

Published By:
Blue Eyes Intelligence Engineering
and Sciences Publication (BEIESP)

III (E). Total chloride contents

Figure 10 represents the variation of total chloride contents of composite cement as well as OPC pastes immersed in Caron's Lake water for 0, 1, 3, 6, 9 and 12 months. The total chloride contents increased with curing time up to 12 months for all hardened cement pastes. This is mainly due to the chemical reaction of Cl- ions with free Portlandite and C_3A as well as C_4AF to produce $CaCl_2$ and calcium chloroaluminate hydrates. The total chloride contents of OPC cement pastes (M0) had higher values than the OPC-GBFS pastes mix M1. OPC pastes (M0) showed the highest value of chlorides due to the increase of liberated lime, which reacted with chloride ions giving calcium chloroaluminate hydrates. The values of total chloride contents of the composite cement pastes have lower values up to 12 months. Composite cement pastes containing NS led to lower Ca^{2+} concentration and porosity to produce a compact structure with very much finer pores, thereby inhibiting the chloride ion penetration **[28]**. The increased gel porosity could result from a higher hydration degree and from the properties of the gel produced by the pozzolanic reaction of NS particles. Pozzolanic C-S-H gels have a lower Ca/Si ratio **[43]**. NS promotes the densification of the cement matrix. Despite this densification, the apparent porosity of paste increases with the addition of NS. This improve the durability of composite cement pastes containing NS, hence the total chloride contents decreased. The accumulation of excessive amounts of hydrates within the open pore systems, due to the highly pozzolanic reaction of NS with liberated CH to produce a more compact structure with very much finer pores, thereby inhibiting the chloride ion penetration; this effect leads to a decrease in the accessibility of chloride towards the more compact structure with low capillary pore structure of the hardened pastes after prolonged hydration. It was found that, blending of OPC with NS is beneficial to the prevention or the decrease of chloride ions diffusion, due to formation of more compact and finer pore structure.

III (F). Total sulphate contents

Figure 11 represents the variation of total sulphate contents of composite cement as well as OPC pastes immersed in Caron's Lake water for 0, 1, 3, 6, 9 and 12 months. The total sulphate contents increased with curing time up to 12 months for all hardened cement pastes. This was due to the immersion of pastes in Caron's Lake water containing sulfate ions forming calcium sulfate dihydrate (gypsum) and a tricalcium sulphoaluminate (ettringite) phase **[24, 27]**. The OPC pastes gave higher values of total sulphate content than those composite cement pastes containing NS up to 12 months; this is due to the higher content of Portlandite. Sulphoaluminate hydrates are formed at early ages of hydration, which need high amount of sulphate ions, precipitate, close the pores and hinder the penetration of more sulphate ions. The total sulphate content increases sharply at one month, then the specimens show gradually increase at the later ages of hydration. The high reactivity and faster pozzolanic activity of NS particles produced a more refined microstructure. Accumulation of excessive amounts of hydrates within the open pore systems to produce a more compact structure with very much finer pores, inhibiting the sulphate ions penetration; leads to decrease the accessibility of sulfate ions towards the more compact structure. Radius of Cl^- ion is smaller the radius of sulphate ion, so the attack of Cl^- ions more effective at all curing ages than the sulphate attack. On the other hand, when NS was added, the cement pastes become almost impermeable to the penetration of SO_4^{2-} ions. This can be explained by the presence of homogeneous micro structure, characterized by compact and small-sized C–S–H gel, which leads to refinement of the microstructure of the paste **[28]**.

III (G). Interpretation of XRD diffraction patterns

Figure 12 illustrates the XRD patterns of M0, M1 and M5 immersed in Caron's Lake water for 0, 1, 6, and 12 months. X-ray diffractograms of composite cement pastes containing different contents of NS show the presence of diffraction lines corresponding to $Ca(OH)_2$, β-C_2S, C_3S, $CaCO_3$ and CSH. XRD peak patterns corresponding to phases (β-C_2S and C_3S) decreases with curing time increases, due to the increase of the hydration process. Calcium chloroaluminate hydrate is not formed during immersion in tap water (0 month). Increase the hydration times, the intensity of the peaks corresponding to the calcium chloroaluminate hydrate increases, whereas the intensity of the peaks corresponding ettringite hydrate decreases. Caron's Lake water contains 12543 ppm Cl^- and 8680 ppm SO_4^{2-} **[24, 27]**; therefore, the effect of chloride on the cement pastes is higher than the effect of sulphate. This is due to the small radius of Cl- in comparison with $SO4^{2-}$. The competition exists between sulphate ions and chloride ions. So, sulphate ions decrease the chloride-binding capability greatly. Obviously, the lower of suphate content of composite cement pastes containing NS is one of the reasons that composite cement containing NS has higher performance to resist the chloride-induced corrosion attack, due to the higher radius of $SO4^{2-}$ ions and their effect on the chloride binding is less **[47]**. The intensity of CH peaks decrease with the increase of NS content, this is due to the pozzolanic reaction of NS with CH to form the additional calcium silicates hydrated phases. XRD diffraction patterns of M5 hydrated showed that the peaks of CH and anhydrous silicate phases (β-C_2S and C_3S) decrease with immersion time up to 12 months. This is due to pozzolanic activity of NS with the liberated CH to form additional hydrated products. These additional hydrated products precipitated in the available open pores to form more compact and closed microstructure with higher stiffness C-S-H. The more compact close structure, inhibiting the $SO4^{2-}$ and Cl^- ions penetration; leads to decrease the accessibility of $SO4^{2-}$ and Cl^- ions towards the more compact structure. The suphates influence the chloride-binding capability, because of the preferential reaction between suphates and C3A. More C_3A reacts with suphates; less C_3A can bind the chloride to form calcium chloroaluminate hydrates. But OH- ion can be exchanged with chloride ion, because the OH^- ion is attracted by the electrovalent bond to form calcium chloroaluminate hydrate as well as structure of C_4AH_{13} can be denoted as $2[Ca_2Al(OH)_6OH.H_2O]$**[48]**. Suphates are more aggressive than chloride, due to that; the chemical bounded chloro-compounds are not expansive.

Published By:
Blue Eyes Intelligence Engineering
and Sciences Publication (BEIESP)

Chloride chemically reacts with the aluminate of hydrated phases of cement such as monosulphates, forming 3 CaO. Al_2O_3. $CaCl_2$. 10 H_2O (Friedel's salt). Another oxychloride compounds (x $Ca(OH)_2$. y $CaCl_2$. z H_2O) can be also formed in the presence of concentrated chloride salts. The presence of chloride limited the sulphate attack, due to the increase of solubility of Portlandite and the formation of hydrated $CaCl_2$ compounds **[49]**.

III (H). Microstructure

Figs.13-15 show SEM micrographs of hardened cement pastes of M0, M1 and M5 immersed in Caron's Lake water for 0, 6 and 12 months. Fig.13 shows SEM micrographs of hardened pastes of M0 immersed in Caron's Lake water for 0, 6 and 12 months. Fig.13 (A) shows a flocculent and porous structure of ill crystalline C-S-H and sheets of massive $Ca(OH)_2$ embedded through regions of C-S-H gel with a wider pores are available for crystallization of the formed hydrates. Fig.13 (B) represented the presence of ettringite needles, hexagonal plates and Friedel's salt within the pore system. Increase the immersion time up to 12 months, hexagonal plates of Friedel's salt and plates of Portlandite growing in pores as shown in Fig.13 (C). Fig.14 shows SEM micrographs of hardened pastes of M1 immersed in Caron's Lake water for 0, 6 and 12 months, respectively. Fig.14 (A) shows porous structure of ill crystalline C-S-H and sheets of massive $Ca(OH)_2$ within the pores. Increase the immersion time NaCl content activates the GBFS pozzolanic reactivity (M1 contains 45 wt., % GBFS), leading to the formation of hydrated aluminates of layered structure as observed in Fig.14(B), which are subsequently transformed into Friedel's salt via OH^-/Cl^- ionic exchange inside the interlayer space **[50]**. Increase the immersion time up to 12 months, hexagonal plates of Friedel's salt and plates of Portlandite growing in pores as shown in Fig.14(C). The microstructural analysis of the hardened composite NS characterized by compact and small-sized C–S–H gel. NS caused a refinement of the microstructure and induced the precipitation of small-sized C–S–H gel, probably having a higher stiffness and lower Ca/Si ratio **[32]**. Fig.15 shows SEM micrographs of hardened pastes of M5 immersed in Caron's Lake water for 0, 6 and 12 months. Fig.15 (A) showed that, the micrograph is composed of dense structure of platelet-like hydrates of C-S-H and crystalline hydrates having close structure with interlocking arrangements. NS has high pozzolanic activity reacted with CH liberated from the cement hydration to form additional C-S-H. The occurrence of C-S-H in large quantity is responsible for bridging cement particles and producing a rigid system. Fig. 15 (B) presents the presence of closed structure arrangement due to precipitation of C-S-H within the wider pores. The micrograph shows also, the paste has a high degree of hydration and lower porosity. After 12 months immersion in Caron's Lake water somewhat hexagonal plates of Friedel's salt and ettringite needles on the surface of wider pore system and absence of sheets of hexagonal plates of Portlandite Fig. 15 (C).

IV. CONCLUSIONS

From the above results it can be concluded that:

1. Initial and final setting times are elongated with NS content, due to the presence of 1% of polycarboxylate superplasticizer as well as the excess of mixing water required for standard consistency.
2. The composite cement paste containing 4 mass% NS (M5) has the highest values of chemically combined water contents cured in Caron's Lake water for 12 months, whereas it decreases with 5-6% NS (M6 and M7), but still higher than M0 and M1 pastes.
3. The Portlandite contents of the OPC pastes decreased with curing time up to 3 months and then increased up to 1 year. As NS content increases, the values of free Portlandite contents and pH values decrease up to 12 months.
4. The compressive strength, flexural strength and bulk density of OPC cement mortar (M0) increased up to 3 months, whereas these values corresponding of mix (M1) increase up to 6 months and then decreased up to 12 months.
5. Mortars containing M5 (4% NS) possess higher values of compressive and flexural strengths than those of the other mortars containing NS.
6. The OPC pastes gave higher values of total sulfate content than those composite cement pastes containing NS up to 12 months.
7. Partial inhibition of chloroaluminate formation and the fine closed microstructure of composite cement containing NS caused an increase of compressive and flexural strengths.

REFERENCES

[1] Heikal M, El. Didamony H, Moustafa MA. Hydration characteristics and physico-chemical and mechanical characteristics of ternary blended system. Si Ind 74, (5-6),155-161, (2009).
[2] Singh NB, Middendorf B. Chemistry of blended cements part-I: Natural pozzolanas, fly ashes and granulated blast furnace slags. Cem Inter 6 (4) (2008) 76–91.
[3] Singh NB, Middendorf B. Chemistry of blended cements part-II: Silica fume, metakaolin, reactive ashes from agricultural wastes, inert materials and non-Portland blended cements. Cem Inter 6 (2009) 78–93.
[4] Mukesh K, Singh SK, Singh NP, Singh NB. Hydration of multicomponent composite cement: OPC–FA–SF–MK. Constr Build Mater 36, (2012), 68–686.
[5] Shi C, Qian J. High performance cementing materials from industrial slags: A review Resour Conserv Recycl 29, (2000), 195–207.
[6] Nazari A, Riahi S. Splitting tensile strength of concrete using ground granulated blast furnace slag and SiO_2 nano-particles as binders. Energy Build 43 (2011) 864–872.
[7] Li C, Sun H, Li L. A review: the comparison between alkali activated slag (Si+Ca) and metakaoline (Si+Al) cements. Cem Concr Res 40 (2010) 1341–1349.
[8] Chen W. Hydration of slag cement: theory, modeling and application. PhD Thesis, University of Twenty; 2007.
[9] Siddique R. Waste Materials and By-Products in Concrete, Springer-Verlag. Berlin (Heidelberg), 2008.
[10] Sanchez F, Sobolev K. Nanotechnology in concrete – a review. Constr Build Mater 24 (2010), 2060–2071.
[11] Said AM, Zeidan MS, Bassuoni MT, Tian Y. Properties of concrete incorporating nano-silica. Constr Build Mater 36 (2012) 838–844.
[12] Skinner LB, Chae SR, Benmore CJ, Wenk HR, Monteiro PJM. Nanostructure of Calcium Silicate Hydrates in Cements. Physical Review Letters (PRL) 104, 195502 (2010) 1-4.
[13] Constantinides G, Ulm F. The nano-granular nature of C-S-H. J Mech Phys Solids 2007; 55:64–90.

Published By:
Blue Eyes Intelligence Engineering and Sciences Publication (BEIESP)

[14] Nili M, Ehsani A, Shabani K. Influence of nano-SiO_2 and micro-silica on concrete performance. In: Proceedings second international conference on sustainable construction materials and technologies, June 28–30, Universita Politecnica delle Marche, Ancona, Italy; (2010).
[15] Singh LP, Karade SR, Bhattacharyya SK, Yousuf MM, Ahalawat S. Beneficial role of nano-silica in cement based materials-A review. Constr Build Mater 47 (2013), 1069-1077.
[16] Heikal M, Abd El-Aleem S, Morsi WM. Characteristics of blended cements containing nano-silica. HBRC Journal (9) (2013), 243–255.
[17] Bjornstrom J, Martinelli A, Matic A, Borjesson L, Panas I. Accelerating effects of colloidal nano-silica for beneficial calcium–silicate–hydrate formation in cement. Chem Phys Lett 392 (2004), 242–8.
[18] Ji T. Preliminary study on the water permeability and microstructure of concrete incorporating nano-SiO_2. Cem Concr Res 35 (2005), 1943–7.
[19] Gaitero JJ, Campillo I, Guerrero A. Reduction of the calcium leaching rate of cement paste by addition of silica nanoparticles. Cem. Concr. Res. 2008; 38: 1112–8.
[20] Belkowitz JS, Armentrout D. An investigation of nano-silica in the cement hydration process. In: Proceeding (2010) concrete sustainability conference, national ready mixed concrete association, USA; (2010), 1–15.

Published By:
Blue Eyes Intelligence Engineering
and Sciences Publication (BEIESP)

[21] Nazari A, Riahi S. The effects of SiO_2 nanoparticles on physical and mechanical properties of high strength compacting concrete. Compos Part B Eng 42 (2011) 570–578.
[22] Sobolev K, Flores I, Hermosillo R. Nanomaterials and nanotechnology for high performance cement composites. In: Proceedings of ACI session on nanotechnology of concrete: recent developments and future perspectives, November 7, Denver, USA; (2006), 91–118.
[23] Wee TH, Suryavanshi AK, Wong SF, Rahman AK. Sulfate resistance of concrete containing mineral admixtures. ACI Material Journal 2000, 97, (5) 536–549.
[24] Abd El.Aziz M, Abd El.Aleem S, Heikal M, El. Didamony H. Hydration and durability of sulphate-resisting and slag cement blends in Caron's Lake water. Cem Concr Res 35 (2005), 1592–1600.
[25] Ghosh SN, Sarkar SL, Harsh S. Progress in cement and concrete, mineral admixtures in cement and concrete. in: M. Moukwa (Ed.), Durability of Silica Fume Concrete, vol. 4, ABI Books, New Delhi, 1993, 467–493.
[26] Amin AM, Ali AH, El-Didamony H. Durability of some Portland cement pastes in various chloride solutions. Zem-Kalk-Gips 50 (3) (1997) 172–177.
[27] Abd-El-Eziz MA, Heikal M. Hydration characteristics and durability of cements containing fly ash and limestone subjected to Qaron's Lake Water. Adv Cem Res 21(3); (2009), 91-99.
[28] Quercia G, Spiesz P, Hüsken G, Brouwers HJH. SCC modification by use of amorphous nano-silica. Cem Concr Compos 45, (2014), 69–81.
[29] Quercia G, Brouwers HJH. Application of nano-silica (nS) in concrete mixtures. In: Gregor Fisher, Mette Geiker, Ole Hededal, Lisbeth Ottosen, Henrik Stang, editors. 8th fib International Ph.D. symposium in civil engineering, June 20–23, Lyngby, Denmark; 2010, 431–6.
[30] Collepardi M, Ogoumah JJ, Skarp U, Troli R. Influence of amorphous colloidal silica on the properties of self-compacting concretes. In: Proceedings of the international conference challenges in concrete construction-innovations and developments in concrete materials and construction, 9-11 September, Dundee, Scotland, UK; 2002, 473–83.
[31] Maghsoudi AA, Arabpour-Dahooei F. Effect of nanoscale materials in engineering properties of performance self-compacting concrete. In: Proceeding of the 7th international congress on civil engineering, Iran; 2007, 1–11.
[32] Khanzadi M, Tadayon M, Sepehri H, Sepehri M. Influence of nano-silica particles on mechanical properties and permeability of concrete. In: Proceedings second international conference on sustainable construction materials and technologies, June 28–30, Universita Ploitecnica delle Marche, Ancona, Italy; 2010, 1–7.
[33] Baomin W, Lijiu W, Lai FC. Freezing resistance of HPC with nano-SiO_2. J Wuhan Univ Technol, Mater Sci 23 (1) (2008), 85–8.
[34] Wei X, Zhang P. Sensitivity analysis for durability of high performance concrete containing nanoparticles based on grey relational grade. Mod Appl Sci 5(4) (2011), 68–73.
[35] ASTM Designation: C191, Standard method for normal consistency and setting of hydraulic cement, ASTM Annual Book of ASTM Standards, (2008).
[36] Abd-El.Aziz MA, Abd.El.Aleem S, Heikal M. Physico-chemical and mechanical characteristics of pozzolanic cement pastes and mortars hydrated at different curing temperatures. Constr Build Mater 26; (2012), 310–316.
[37] El-Didamony H, Heikal M, Abd. El. Aleem S. Influence of delayed addition time of sodium sulfanilate phenol formaldehyde condensate on the hydration characteristics of sulfate resisting cement pastes containing silica fume. Constr Build Mater 37; (2012), 269–276.
[38] ASTM C109, Strength test method for compressive strength of hydraulic cement mortars, (2007).
[39] Heikal M, Aiad I, Helmy IM. Portland cement clinker, granulated slag and by-pass cement dust composites. Cem Concr Res 32, (2002)1809-1812.
[40] Qing Y, Zenan Z, Deyu K, Rongshen C. Influence of nano-SiO_2 addition on properties of hardened cement paste as compared with silica fume. Constr Build Mater 2007; 21:539–45.
[41] Land G, Stephan D. The influence of nano-silica on the hydration of ordinary Portland cement. J. Mater. Sci. 47 (2012), 1011–1017.
[42] Jalal M, Mansouri E, Sharifipour M, Pouladkhan AR. Mechanical, rheological, durability and microstructural properties of high performance self-compacting concrete containing SiO_2 micro and nanoparticles. Mater Des, 2012;34:389–400.
[43] Lotenbach B, Scrivener K, Hooton RD. Supplementary cementitious materials. Cem Concr Res 2001;41:1244–56.
[44] Bonen D, Cohen MD. Magnesium sulphate on Portland cement paste: II. Chemical and mineralogical analysis. Cem Concr Res 22, (1992) 707-718.
[45] Ali AH, El-Didamony H, Mostafa KA. Sea water attack on sulfate resisting cement containing granulated slag and silica fume. Silicates Industrials; Ceramic Science and Technology. 1997, 62, (11–12), 199–203.
[46] Mondal P, Shah SP, Marks LD, Gaitero JJ. Comparative study of the effects of microsilica and nanosilica in concrete. Transportation Research Record: Journal of the Transportation Research Board, No. 2141. Washington, DC: Transportation Research Board of the National Academies; 2010, 6–9.
[47] Luo R, Cai Y, Wang C, Huang X. Study of chloride binding and diffusion in GGBS concrete. Cem Concr Res, 33 (2003) 1-7.
[48] Lea FM, the Chemistry of Cement Concrete, China Construction Industry Publishing House, Beijing, 1980, 256– 290.
[49] Glasser FP, Marchand J, Samson E. Durability of concrete – degradation phenomena involving detrimental chemical reactions. Cem Concr Res 2008; 38:226–46.
[50] Goñi S, Lorenzo MP, Sagrera JL. Durability of hydrated Portland cement with copper slag addition in NaCl + Na_2SO_4 medium. Cem Concr Res 1994; 24(8):1403–12.

Table 1: Chemical analysis of OPC, GBFS and NS, (mass %)

	SiO_2	Al_2O_3	Fe_2O_3	CaO	MgO	SO_3	Na_2O	K_2O	L.O I.	Total
OPC	21.30	3.58	5.05	63.48	1.39	2.05	0.26	0.22	2.57	99.90
GBFS	43.21	9.97	0.59	35.96	5.43	1.37	0.79	0.67	1.98	99.97
NS	88.61	0.01	0.01	0.01	0.01	0.29	0.04	0.29	--	--

Published By:
Blue Eyes Intelligence Engineering
and Sciences Publication (BEIESP)

ISSN: 2249-8958 (Online), Volume-4 Issue-6, August 2015

Table 2: Mix composition of OPC and composite cements in mass, %

Mix No.	OPC	GBFS	NS
M0	100	0	0
M1	55	45	0
M2	54	45	1
M3	53	45	2
M4	52	45	3
M5	51	45	4
M6	50	45	5
M7	49	45	6

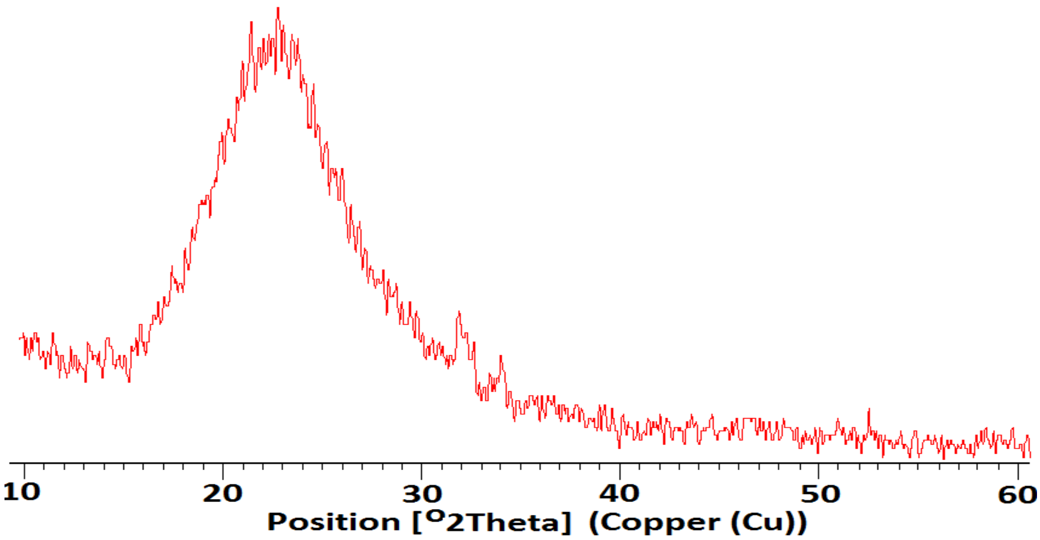

Fig. 1: XRD of nano-silica

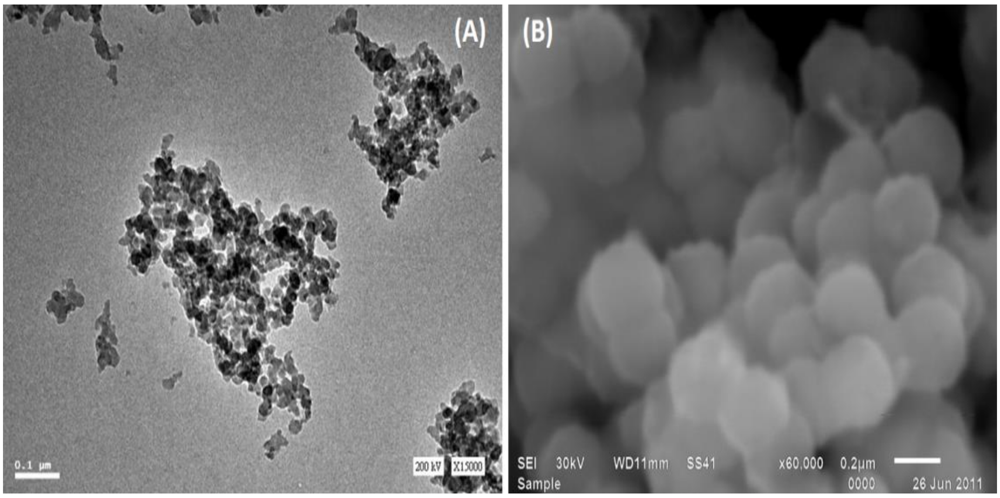

Fig. 2: (A) TEM and (B) SEM photographs of nano-silica

Published By:
Blue Eyes Intelligence Engineering
and Sciences Publication (BEIESP)

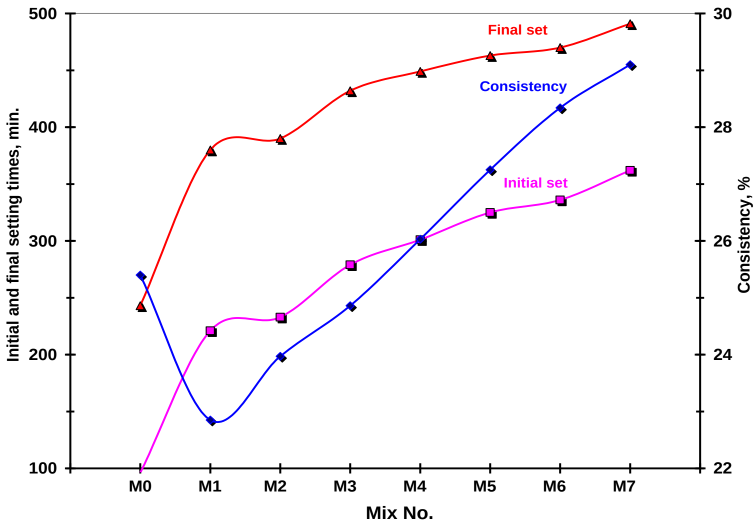

Fig. 3: Water of consistency, initial and final setting times of OPC-GBFS-NS pastes

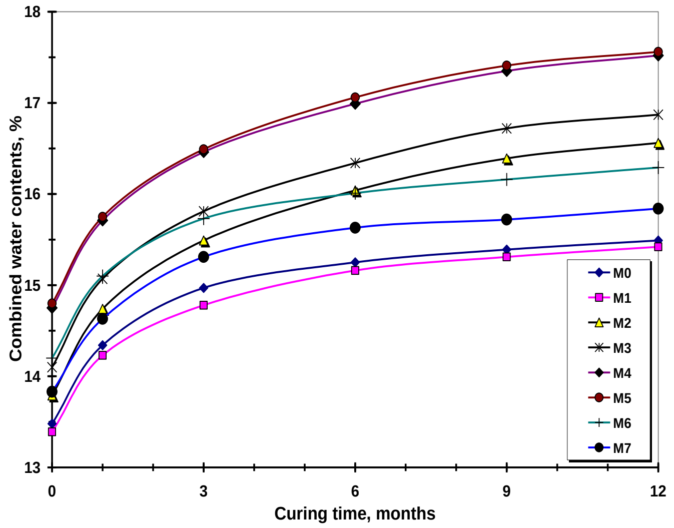

Fig. 4: Combined water contents of OPC-GBFS-NS pastes immersed in Caron's Lake water up to 1 year

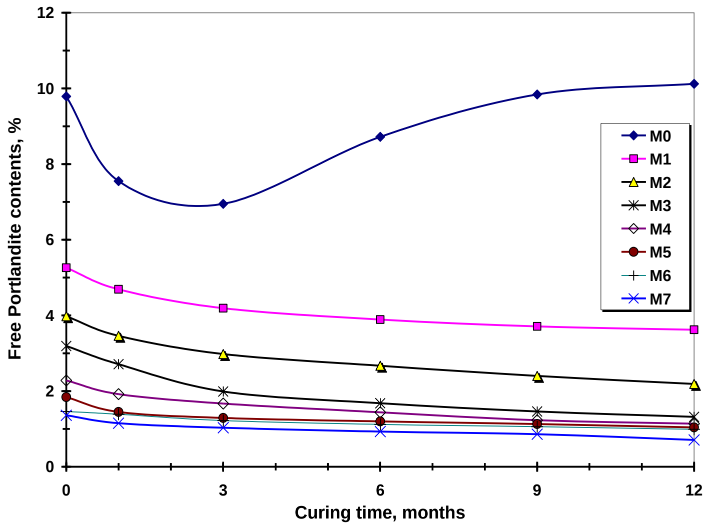

Fig. 5: Free lime contents of OPC-GBFS-NS pastes immersed in Caron's Lake water up to 1 year

Published By:
Blue Eyes Intelligence Engineering
and Sciences Publication (BEIESP)

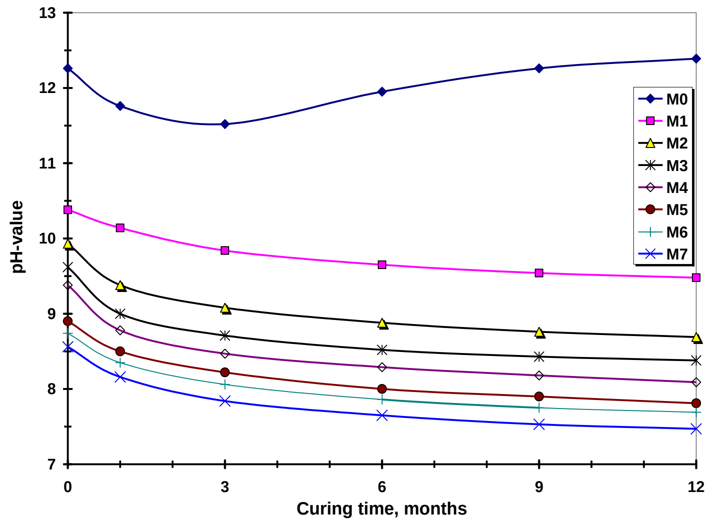

Fig. 6: pH values of OPC-GBFS-NS pastes immersed in Caron's Lake water up to 1 year

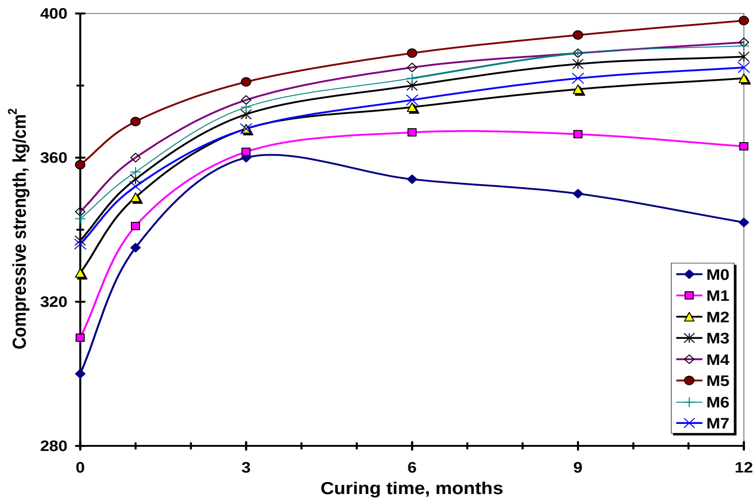

Fig. 7: Compressive strength of OPC-GBFS-NS mortars immersed in Caron's Lake water up to 1 year

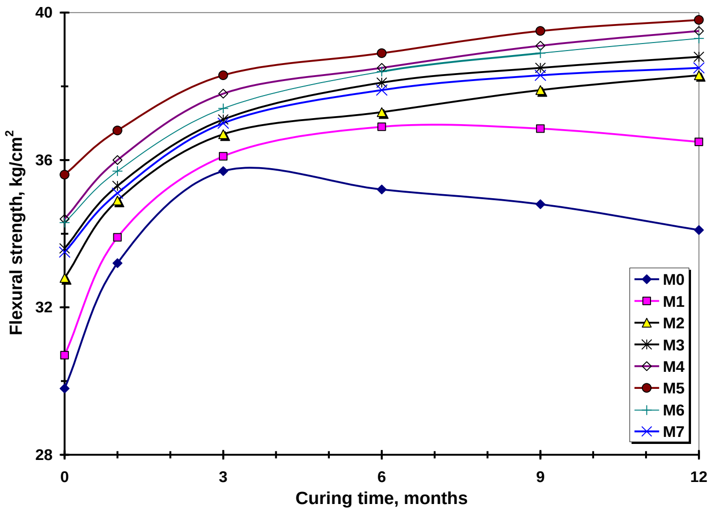

Fig. 8: Flexural strength of OPC-GBFS-NS cement mortars immersed in Caron's Lake water up to 1 year

Published By:
Blue Eyes Intelligence Engineering
and Sciences Publication (BEIESP)

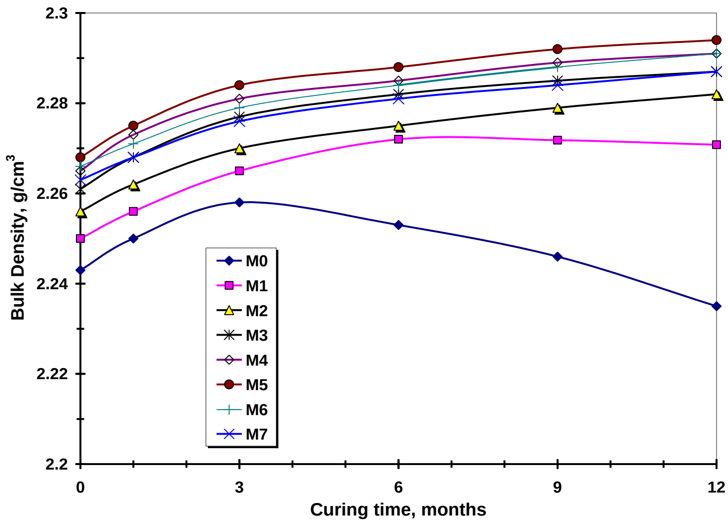

Fig. 9: Bulk density of OPC-GBFS-NS mortars immersed in Caron's Lake water up to 1 year

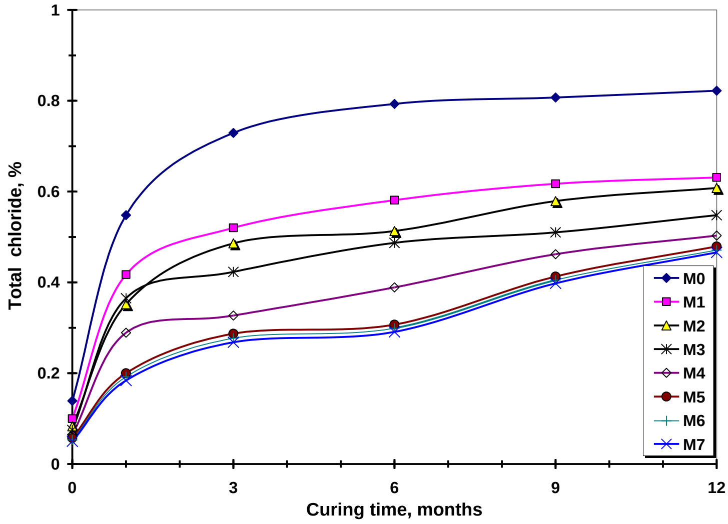

Fig. 10: Total chloride contents of OPC-GBFS-NS pastes immersed in Caron's Lake water up to 1 year

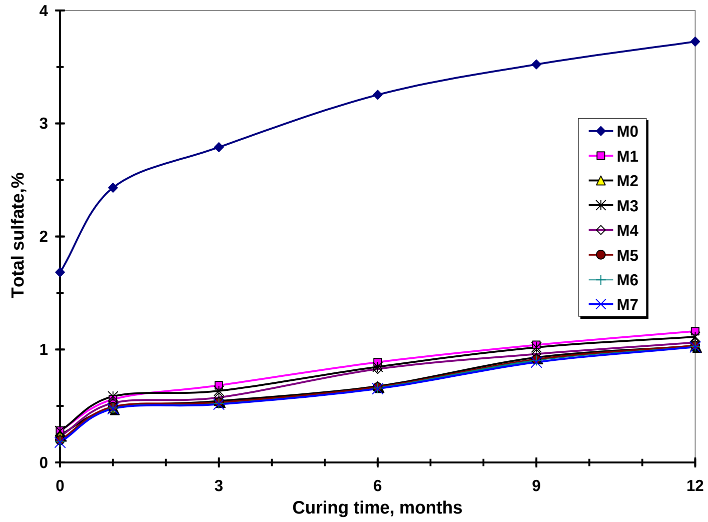

Fig. 11: Total sulphate contents of OPC-GBFS-NS pastes immersed in Caron's Lake water up to 1 year

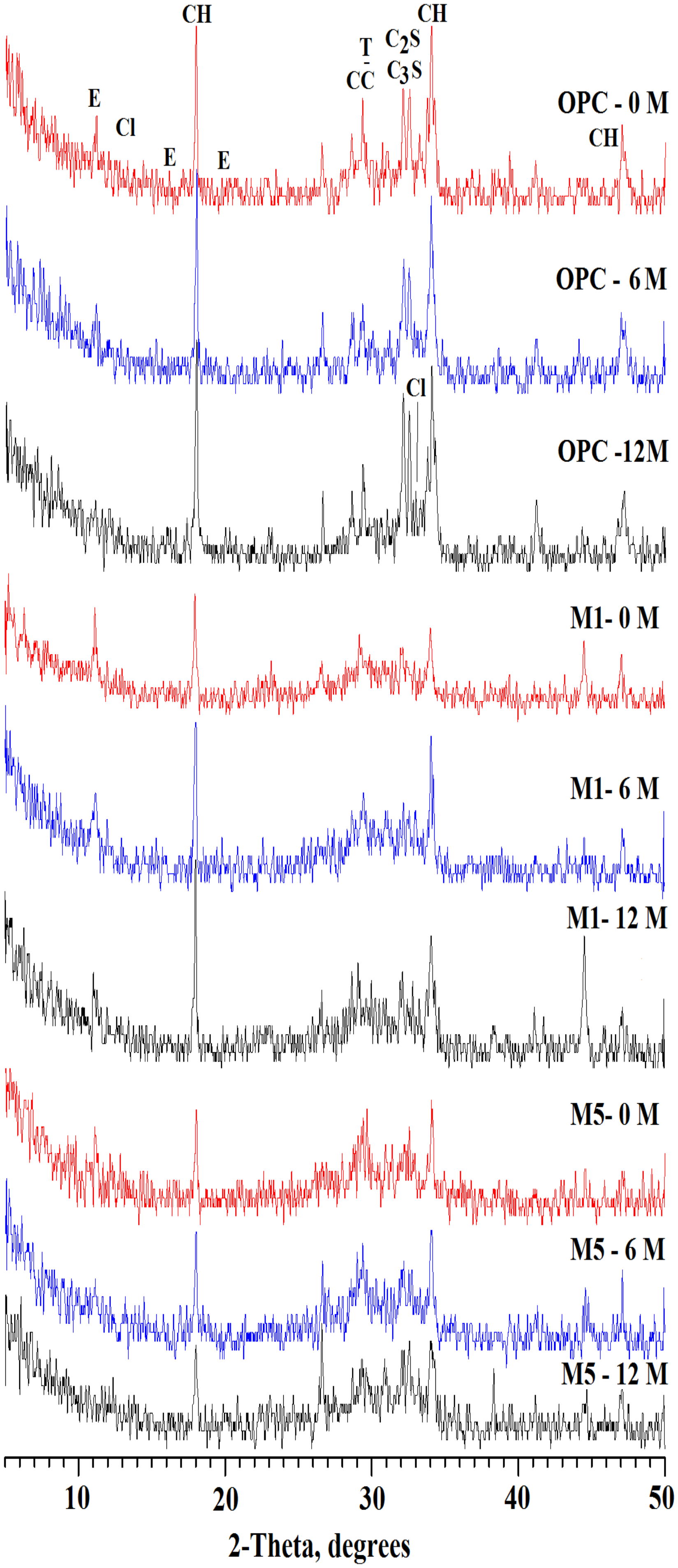

Published By:
Blue Eyes Intelligence Engineering
and Sciences Publication (BEIESP)

Fig. 12: XRD patterns of M0, M1 and M5 immersed in Caron's Lake water for 0, 6 and 12 months

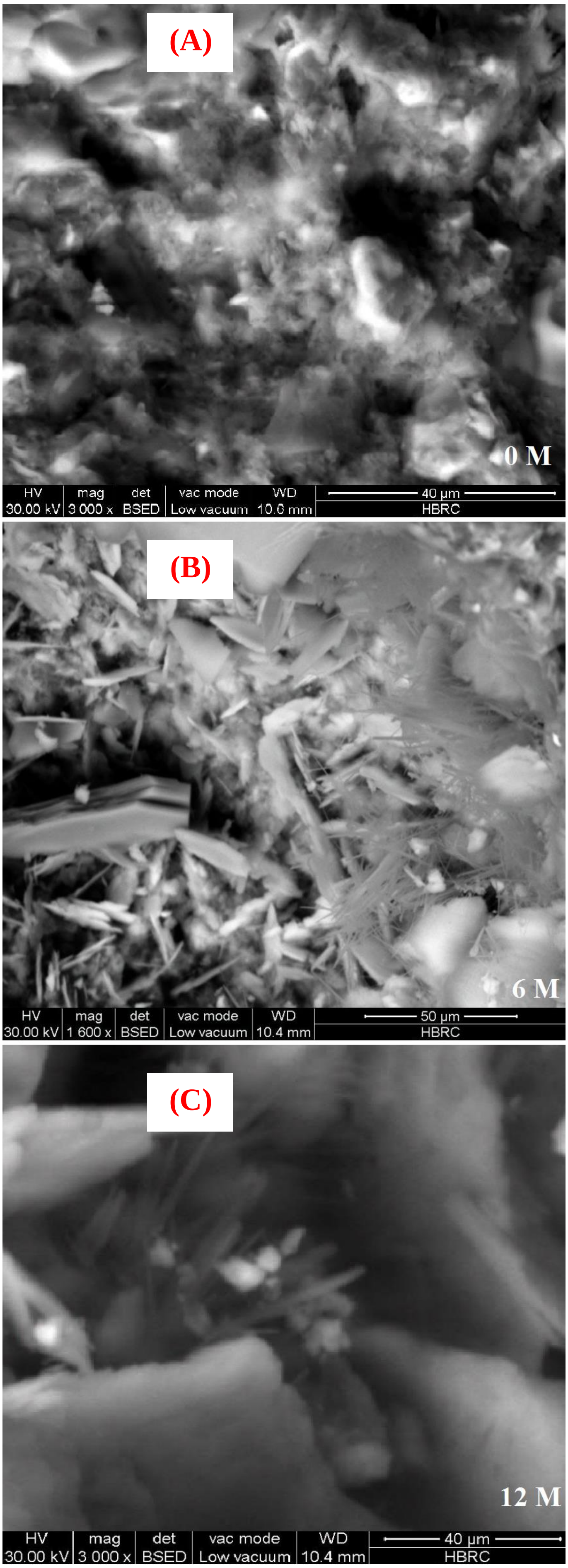

Published By:
Blue Eyes Intelligence Engineering
and Sciences Publication (BEIESP)

Fig. 13 (A& B &C): SEM micrographs of M0 immersed in Caron's Lake water for 0, 6 and 12 months, respectively

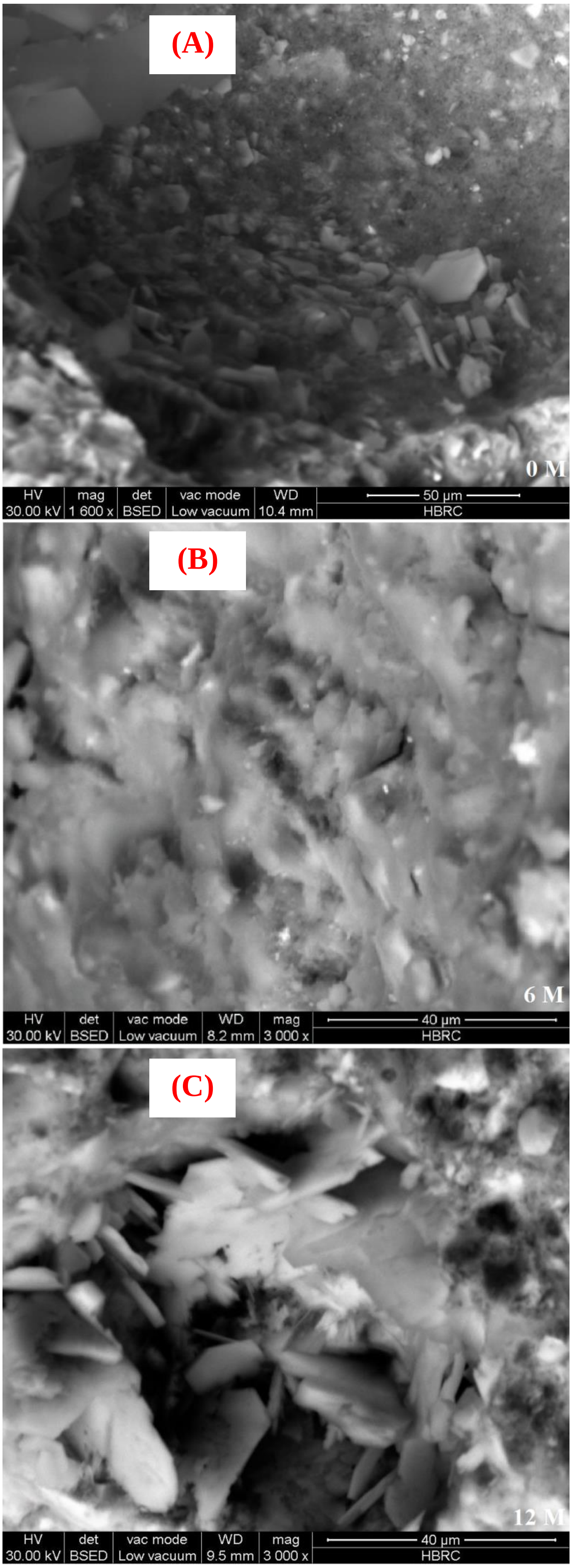

Published By:
Blue Eyes Intelligence Engineering
and Sciences Publication (BEIESP)

Fig. 14 (A& B &C): SEM micrographs of M1 immersed in Caron’s Lake water for 0, 6 and 12 months, respectively

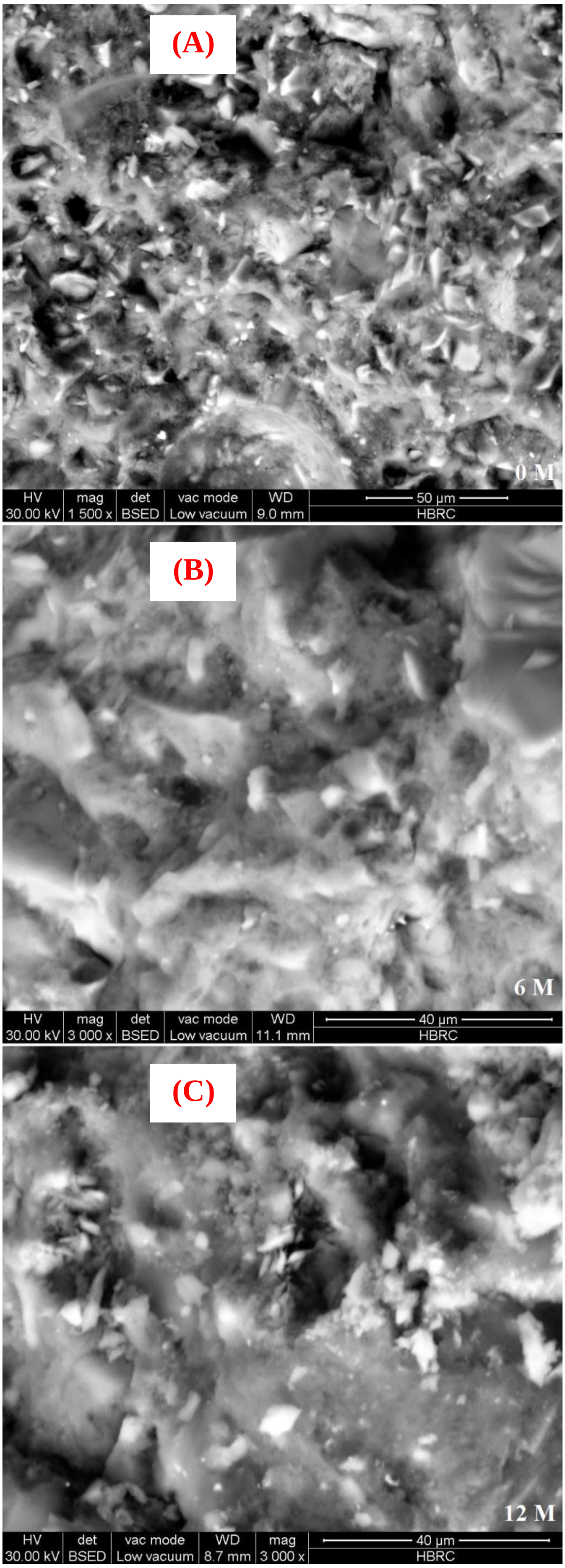

Published By:
Blue Eyes Intelligence Engineering
and Sciences Publication (BEIESP)

Fig. 15 (A& B &C): SEM micrographs of M5 immersed in Caron's Lake water for 0, 6 and 12 months, respectively

Published By:
Blue Eyes Intelligence Engineering
and Sciences Publication (BEIESP)